Electrokinetic instability mechanism of double-layered miscible fluids with different electrolyte concentrations in DC electric field

Jae W. Park*, Kwan H. Kang** and Kang Y. Huh***

*Department of Mechanical Engineering,
Pohang University of Science and Technology, San 31, Hyoja-dong, Pohang 790-784, Republic of Korea,
*slam@postech.ac.kr, **khkang@postech.ac.kr, ***huh@postech.ac.kr

ABSTRACT

Numerical investigation is performed on the electrokinetic instability mechanism of double-layered miscible fluids in DC electric field. Nonlinear interfacial waves as observed in flow visualization are successfully reproduced. The mechanism is explained on the basis of instantaneous velocity vectors, electric field, net charge distributions as well as concentration distributions. Counterclockwise vortical motion is produced according to the directions of concentration gradient and electric field. A strong vortex at the junction of a T-channel may allow fast mixing in high electric field. Simulation well reproduces the qualitative characteristics of instability, while the threshold instability criterion is underestimated.

Keywords: electrokinetic instability, electroosmotic flow

1 INTRODUCTION

Interfacial instability has recently been observed by Chen and Santiago [1] in electroosmotic flow of two miscible layers with different concentrations in a T-channel. Such instability needs to be suppressed in some micro-fluidic systems requiring stable transport with little species dispersion [2]. On the other hand, it can be utilized to enhance mixing of heterogeneous fluids against viscous dissipation at an extremely low Reynolds number. This instability was first found in a case with no mean flow motion by Hoberg and Melcher [3]. The difference is in the electroosmotic flow, which leads to convective instabilities. It has been suggested that the flow instability originates from the polarization due to concentration gradient in imposed electric field and the stability criterion is mapped for the first time through linear stability analysis [4]. The mechanism of the interfacial electrokinetic instability is elucidated numerically by the Nernst–Planck framework of transport equations in this study.

2 FORMULATION

We consider time-dependent mixing of the electrolyte layers flowing into a two-dimensional micro T-channel. The concentrations of the two inflowing streams are denoted as c_h and c_l, in which the subscripts h and l represent the high and low concentration. The electrolytes are free from chemical reaction. For simple analysis unit activity coefficient and uniform dielectric constant of the solution are assumed throughout the domain. The unsteady Navier–Stokes equation with Coulombic body force for incompressible fluid is written as

$$\rho \frac{D\mathbf{u}}{dt} = -\nabla p + \mu \nabla^2 \mathbf{u} + \rho_e \mathbf{E} \tag{1}$$

where $D/Dt = \partial/\partial t + \mathbf{u}\cdot\nabla$, $\mathbf{u} = (u, v, w)$ is velocity vector, t is time, p is hydrodynamic pressure, ρ is mass density and μ is viscosity of fluid. $\mathbf{E} = -\nabla\phi$ is electric field and ϕ is electrostatic potential. The electrostatic potential ϕ is related with the charge density (ρ_e) as

$$\nabla^2 \phi = -\frac{\rho_e}{\varepsilon} \tag{2}$$

where ε is electric permittivity. The charge density is a sum of the concentrations of all species, i.e., $\rho_e = F\sum_i z_i c_i$, in which i = 1 and 2 respectively denote positive ions (cations) and negative ions (anions). c_i is molar concentration (mol/m^3).

The electroosmotic flow on the wall is characterized by the Helmholtz–Smoluchowsi slip velocity given as $u_w = (\varepsilon\zeta/\mu)E_t$. E_t is the tangential electric field on the wall and ζ is the zeta potential of the wall. Here, we exclude the flow in the electrical double layer while the osmotic velocity is imposed as a boundary condition on the wall ($u_t = u_w = -(\varepsilon\zeta/\mu)\nabla\phi$). Uniform average velocities are assumed at both inlets of the T-channel. Conservation of electrical charge can be written in the absence of chemical reaction as

$$\frac{\partial \rho_e}{\partial t} + \nabla\cdot\mathbf{J} = 0 \tag{3}$$

in which the current density is $\mathbf{J} = F\sum_i z_i \mathbf{N}_i$. Assuming Fickian diffusion, the flux density of each species $\mathbf{N}_i$ is expressed according to the following Nernst–Planck relation:

$$\mathbf{N}_i = D_i \nabla c_i + \frac{z_i F D_i}{RT} c_i \mathbf{E} + c_i \mathbf{u} \tag{4}$$

where D_i is diffusivity of ionic species (m^2/s), z_i is the valence of ionic species and F is the Faraday constant. Here we introduce the electroneutrality assumption as

$$\rho_e = F\sum_i z_i c_i \approx 0 \tag{5}$$

The first term in Eq. (3) is neglected on the basis of this assumption. Equation (5) has been validated for various electrochemical systems both numerically and experimentally. For instance, Riveros [5] showed its validity when $\kappa_l d > 20$, where κ_l^{-1} is the Debye length for the dilute solution. This condition is readily satisfied for the present system of interest, in which $\kappa_l d$ is normally greater than 10^2. Substituting Eq. (4) into Eq. (3), we obtain

$$\nabla \cdot (\sigma \nabla \phi) = -F \sum_i z_i \nabla \cdot (D_i \nabla c_i) \tag{6}$$

where

$$\sigma = F^2 \sum_i z_i^2 \omega_i c_i \tag{7}$$

Equation (6) can be rewritten as

$$\nabla^2 \phi = \nabla \sigma \cdot \mathbf{E} - F \left(\sum_i z_i D_i \right) \nabla^2 c \tag{8}$$

Under the electroneutrality assumption, the transport equations for positive and negative species become

$$\frac{Dc}{Dt} = D_1 \nabla^2 c + \frac{zFD_1}{RT} \nabla \cdot (c \nabla \phi) \tag{9a}$$

$$\frac{Dc}{Dt} = D_1 \nabla^2 c - \frac{zFD_2}{RT} \nabla \cdot (c \nabla \phi) \tag{9b}$$

which yield the following convective-diffusion equation for c

$$\frac{Dc}{Dt} = D_{eq} \nabla^2 c \tag{10}$$

D_{eq} is the equivalent diffusivity defined as

$$D_{eq} = \frac{\omega_1 D_2 + \omega_2 D_1}{\omega_1 + \omega_2} = \frac{2 D_1 D_2}{D_1 + D_2}$$

We will solve Eq. (6) rather than the Poisson equation to obtain the charge density. In general it is not a simple problem to solve the transport equations for all species in combination with the Poisson equation. Here with 1:1 symmetric electrolytes, the conductivity in Eq. (7) becomes

$$\sigma = \frac{F^2}{RT} (D_1 + D_2) c \tag{11}$$

If we replace the conductivity with the concentration by Eq. (11), all the equations may now be written as

$$\rho \frac{D\mathbf{u}}{Dt} = -\nabla p + \mu \nabla^2 \mathbf{u} + \varepsilon (\nabla^2 \phi) \nabla \phi \tag{12}$$

$$\nabla \cdot (c \nabla \phi) = -\frac{RT}{F} \frac{(D_1 - D_2)}{(D_1 + D_2)} \nabla^2 c \tag{13}$$

$$\frac{Dc}{Dt} = D_{eq} \nabla^2 c \tag{14}$$

These governing equations are non-dimensionalized by introducing the following variables:

$$\bar{t} = \frac{t}{t_c}, \quad \bar{x} = \frac{x}{d}, \quad \bar{y} = \frac{y}{d}, \quad \bar{\mathbf{E}} = \frac{\mathbf{E}}{E_o}, \quad \bar{\phi} = \frac{\phi}{E_o d}, \quad \bar{\mathbf{u}} = \frac{\mathbf{u}}{u_c}, \quad \bar{c} = \frac{c}{c_h - c_l}, \quad \bar{\rho}_e = \frac{\rho_e}{\varepsilon (E_o / d)} \tag{15}$$

where $t_c = d / u_c$ and the characteristic velocity is taken as the electroosmotic Helmholtz–Smoluchowski slip velocity ($u_c = \varepsilon E_o \zeta / \mu$). Substituting the dimensionless variables in Eqs. (1), (6) and (10), we obtain the following non-dimensional equations. The overbar is dropped for brevity of the notations.

$$\frac{D\mathbf{u}}{Dt} = -\nabla p + \frac{1}{\mathrm{Re}} \nabla^2 \mathbf{u} + \lambda (\nabla^2 \phi) \nabla \phi$$

$$\nabla \cdot (c \nabla \phi) = G \nabla^2 c$$

$$\frac{Dc}{Dt} = \frac{1}{Pe} \nabla^2 c$$

The dimensionless parameters are defined as

$$\mathrm{Re} = \frac{u_c d}{\nu} = Pe \frac{D_{eq}}{\nu} = \frac{Pe}{Sc}, \; Sc = \frac{\nu}{D_{eq}}, \; Pe = \frac{u_c d}{D_{eq}} = \frac{\varepsilon E_o \zeta d}{\mu D_{eq}}$$

$$G = \left(\frac{D_2 - D_1}{D_1 + D_2} \right) \frac{1}{\beta E_o d} = \frac{\alpha_2 - \alpha_1}{\beta E_o d}, \; \lambda = \frac{\varepsilon E_o^2}{\rho u_c^2} = \frac{\mu^2}{\rho \varepsilon \zeta^2}$$

where $\beta = ze / kT$, which becomes $39\mathrm{V}^{-1}$ for z = 1. κ is the inverse Debye length defined as

$$\kappa^2 = \frac{F^2 (c_{h0} - c_{l0})}{\varepsilon RT} \tag{16}$$

3 RESULT AND DISSCUSSION

3.1 Mechanism of instability

By substituting the Poisson equation into Eq. (6) the charge density is expressed as

$$\frac{\rho_e}{\varepsilon} = -\frac{\nabla \sigma \cdot \mathbf{E}}{\sigma} + \frac{F}{\sigma} \left(\sum_i z_i D_i \right) \nabla^2 c \tag{17}$$

which describes how free charges are produced. The first term on the right-hand side is the contribution from concentration gradient. The strength of electric field decreases, if the current flows from high conductivity region to the region of low conductivity as in Fig. 1(a). Negative charges are generated to satisfy the Gauss' law in the domain, while the Coulombic force acts to the left in this case. The conductivity gradient is reversed in Fig. 1(b) with the electric field increasing in the current direction. Positive charges are produced to be forced to the right in Fig. 1(b). The second term on the right hand side of Eq. (17) represents the contribution from diffusivity difference of ionic species, which is related with the liquid junction potential. This term is usually much smaller than the first term.

Numerical simulation is performed for the case close to Chen and Santiago [1]. Let us consider the case of aqueous NaCl solution in a microchannel with the width of d = 150 μm. The electrolyte concentrations are chosen to be c_l = 1 mM and c_h = 10 mM, respectively. Then, the zeta potential becomes ζ_l = 55.2 mV and ζ_h = 34.2 mV. The diffusivities of Na^+ and Cl^- ions in a dilute solution are 1.33×10^{-9} m^2/s and 2.03×10^{-9} m^2/s, respectively. Then it follows that $D_{eq} = 1.607 \times 10^{-9}$ and $\alpha_1 - \alpha_2 = -0.21$. In the experiment the applied potential difference is from 0.5 kV to 3.0 kV and the channel length is about 2.6 cm. The

electric fields E_o in the unperturbed regions of the upper and lower branches are estimated to be from 16,025 V/m to 96,153 V/m according to the applied voltages. In the case of the threshold voltage 0.9 kV, the estimated Helmholtz–Smoluchowski slip velocity for each stream is u_h = 1.15 mm/s and u_l = 0.711 mm/s, thus u_c = 0.93 mm/s, Re = 0.14, Pe = 86.8, G = 1.1×10^{-3}, Sc = 598, and λ = 832.

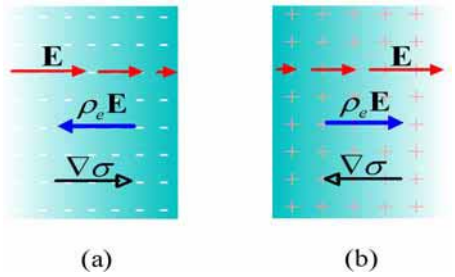

FIG. 1 Polarization due to conductivity gradient. Darkness level indicates the concentration.

Figure 2(a) shows the calculated concentration distribution for a typical case. The interface pattern is almost identical with that observed in experiment. Figure 2(b) shows the distribution of charge density together with the concentration distribution in solid lines. Darker regions have dominant positive charges, while brighter regions have dominant negative charges. The Coulombic force is proportional to $\rho_e\mathbf{E} \sim -(1/c)(\nabla c\cdot\mathbf{E})\mathbf{E}$. The growth of the interface pattern can be divided into two stages according to the charge production mechanism. In the first stage the species diffusion across the interface plays a crucial role. Molecular diffusion increases the thickness of the mixing layer in the flow direction. The gradient, $\partial c/\partial x$, is nonzero, so that ρ_e becomes nonzero in the thin mixing zone. $\partial c/\partial x > 0$ ($\partial c/\partial x < 0$) at the upper (lower) part of the mixing layer. Accordingly, ρ_e is negative (positive) above (below) the center region. Since the magnitude of ρ_e is proportional to $(1/c)$, the negative ρ_e in the upper part is more apparent in Fig. 2(b). Although not shown here, the vertical component of **E** is much smaller that the horizontal component, just after the junction region of the channel. Then, the Coulombic force generates counter-clockwise vortices at the mixing layer with subsequent development of the wavy interface pattern.

The later stage of growth originates from nonlinear deformation of the interface. Once the mixing layer forms a hump (which is convex upward), $\rho_e \sim -\nabla c\cdot\mathbf{E}/c < 0$ at the back of the hump while $\rho_e \sim \nabla c\cdot\mathbf{E}/c < 0$ at the fore of the hump. As a result negative and positive charges are induced periodically at the back and fore of each hump in Fig. 2(b). The flow is either decelerated or accelerated depending on the sign and magnitude of induced charges due to the Coulombic force. Downstream flow velocity is decreased at the back of each hump (P1 to P4), while increased at the fore region (P5 to P8) in Figure 2(c). Decreasing flow velocity (due to the dragging effect of the Coulombic force) at P1 to P4 primarily contributes to formation of the unstable interface pattern. The spike pattern grows downstream, since the induced charge increases with deformation of the interface. The growth is limited by the stabilizing effect of molecular diffusion and the bounding effect of the channel wall.

Note that the electrokinetically generated vorticity is always in the counterclockwise direction. Consequently, the growing spikes form always in the backward direction, which is consistent for all experimental observations.

3.2 Mixing enhancement in high electric field

Diffusion is the only effective mixing mechanism for low Reynolds number laminar flow in a microchannel. There have been many trials to enhance mixing by complicated flow patterns of conventional passive mixers or external forces of active mixers. For instance, Hau et al. [6] showed that surface charges under steady electric field can drive unstable vortical motion enhancing mixing in electroosmotic flow. Here we consider similar, but much stronger and controllable vortical motion due to concentration gradients in applied electric field.

Figure 3(a) shows visualization in experiment at an applied electric field of 1.47×10^5 V/m. As the interface between two different concentration fluids is retreated to the direction of the lower entrance it seems that the stream of the higher concentration is choked at the lower corner of the junction. The concentration image reveals fast mixing of the two streams within a short distance. Figure 3(b) shows the calculated concentration profiles with instantaneous velocity vectors. It is clear that a strong counterclockwise vortex is located at the center of the T-junction, where the flow from the upper inlet meets that from the lower inlet. To satisfy the continuity relationship, a velocity vector around the vortex should have a considerable y-component yielding strong convective diffusion. The downstream concentration profile confirms fast and effective mixing, although weak molecular diffusion follows further downstream. To augment mixing, this instability mechanism may be combined with pressure-driven flow or the conductivity may be controlled by adding some salt to one of the fluids. This type of mixing mechanism can be beneficial in many practical application, since it does not involve any complex physical structures.

CONCLUDING REMARK

The detailed mechanism of electrokinetic instability for two miscible fluids of different concentrations is clarified from the calculation results of flow velocity, electric field and concentration distributions. It is suggested as an effective strategy for micro mixers to utilize the unstable vortex motion to enhance mixing of heterogeneous fluids with considerable concentration differences. Relevant experimental work is under progress.

REFERENCES

[1] C. H. Chen and J. G. Santiago, "Electrokinetic flow instability in high concentration gradient microflows," Proc. 2002 Int. Mech. Eng. Cong. and Exp., New Orleans, LA, CD vol.1, Paper No. 33563. 2002.

[2] S. C. Jacobson and J. M. Ramsey, "Electrokinetic focusing in microfabricated channel structures," Analytical Chemistry, vol. 69, No. 16, pp. 3212-3217, 1997.

[3] J. F. Hoberg and J. R. Melcher, "Internal electrohydrodynamic instability and mixing of fluids with orthogonal field and conductivity gradients," J. Fluid Mech. Vol. 73, pp. 333-351, 1976.

[4] C. H. Chen, H. Lin, S. K Lele and J. G. Santiago, "Electrokinetic microflow instability with conductivity gradients," 7th int. conf. on μTAS, Oct 5-9, Squaw Valley, California, USA, pp. 983-987, 2003.

[5] O. J. Riveros, "Numerical solutions for liquid-junction potentials," J. Phys. Chem., Vol. 96, pp. 6001-6004, 1992.

[6] W. L. W. Hau, L. M. Lee, Y.K. Lee and Y. Zohar, "Electrokinetically-driven vertical motion for mixing of liquids in a microchannel," 7th Int. Conf. on μTAS, Oct 5-9, Squaw Valley, California, USA, pp. 491-494, 2003.

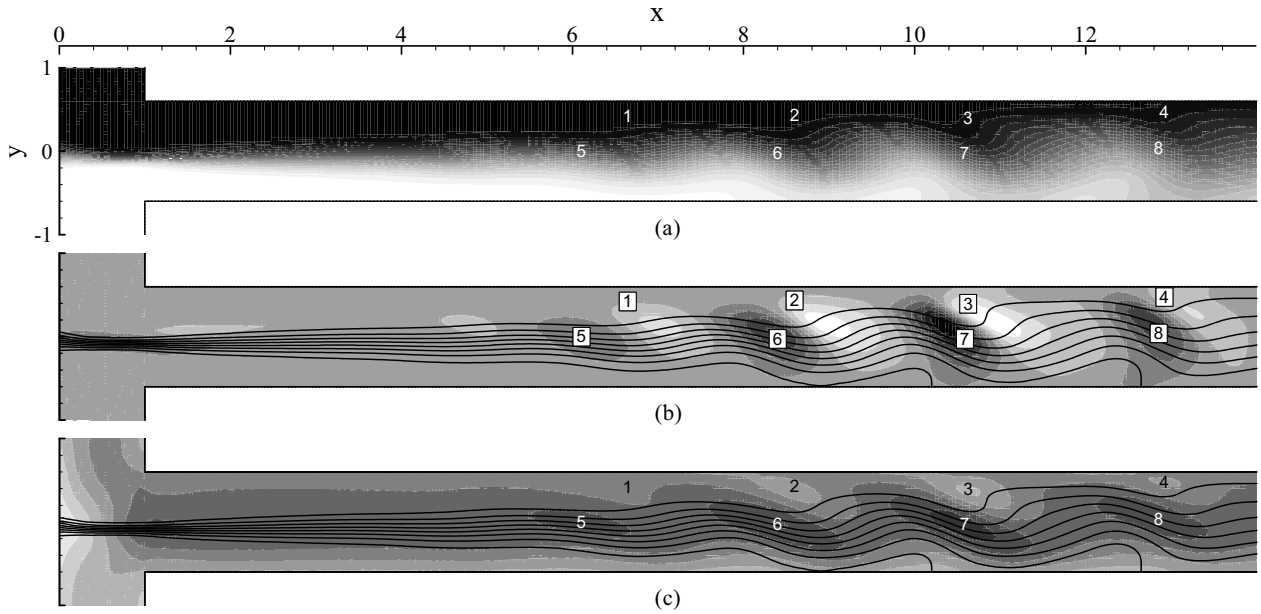

FIG. 2 Numerical results at an instant for $\lambda = 130$. (a) Concentration distribution. (b) Charge density with concentration distribution. (c) Total velocity (darkness level is proportional to velocity magnitude) and iso-concentration lines (line).

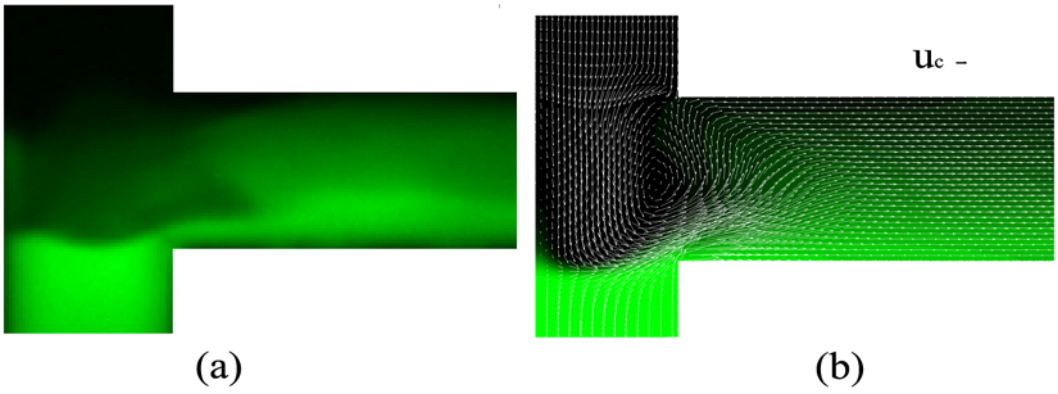

FIG. 3 Concentration profiles in case of high electro static field, (a) experimental result in case of 2.5 kV applied voltage; photo courtesy of S. M. Shin, (b) numerical result with instantaneous velocity vectors in case of λ=200.